SUPPORTING INFORMATION

Manuscript title: **The first study about the relationship between the extractability of thiacalix[4]arene derivatives and the position of the coordination binding sites†**

Author(s): Jiang-Lin Zhao,[a] Hirotsugu Tomiyasu,[a] Xin-Long Ni,[b] Xi Zeng,[b] Mark R. J. Elsegood,[c] Carl Redshaw[d] Shofiur Rahman,[e] Paris E. Georghiou[e] and Takehiko Yamato*[a]

[a] Department of Applied Chemistry, Faculty of Science and Engineering, Saga University, Honjo-machi 1, Saga 840-8502 Japan, E-mail: yamatot@cc.saga-u.ac.jp.

[b] Department Key Laboratory of Macrocyclic and Supramolecular Chemistry of Guizhou Province, Guizhou University, Guiyang, Guizhou, 550025, China.

[c] Chemistry Department, Loughborough University, Loughborough, LE11 3TU, UK.

[d] Department of Chemistry, The University of Hull, Cottingham Road, Hull, Yorkshire, HU6 7RX, UK.

[e] Department of Chemistry, Memorial University of Newfoundland, St. John's, Newfoundland and Labrador, Canada A1B3X7.

Table of Contents

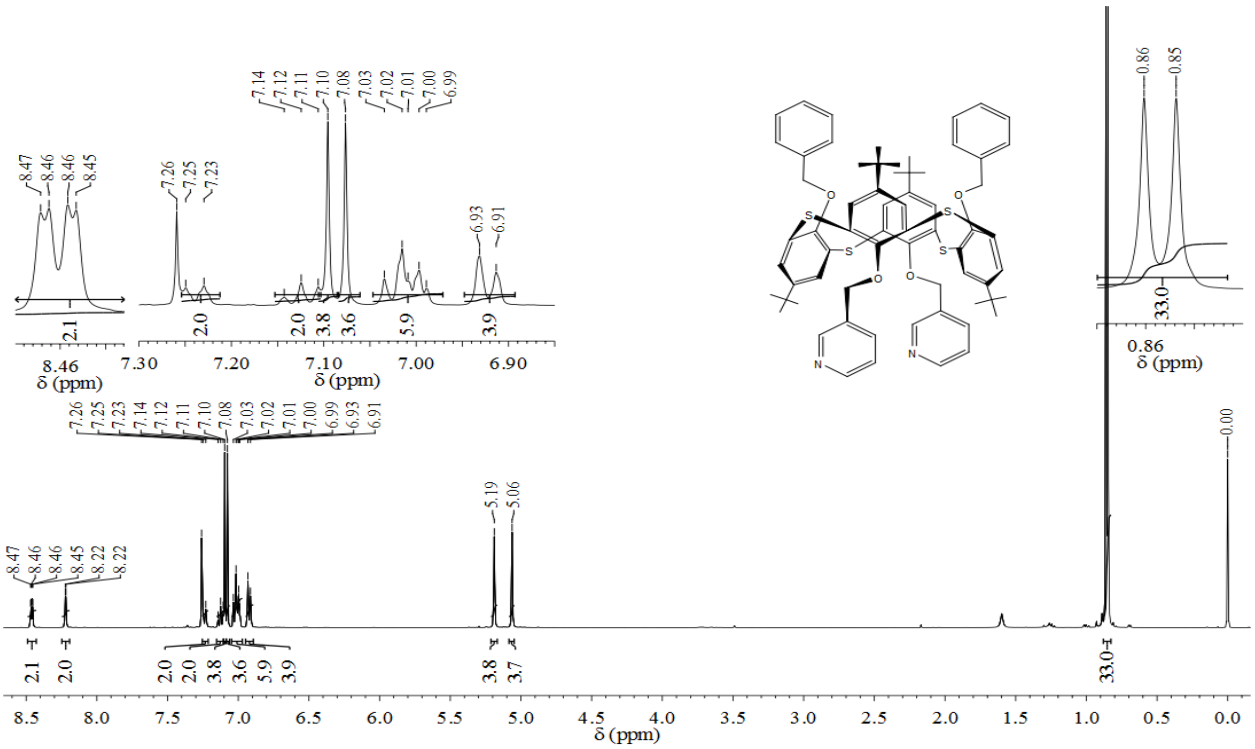

Figure S1. ^{1}H–NMR spectrum of compound **3** (400 MHz, $CDCl_3$, 293 K).

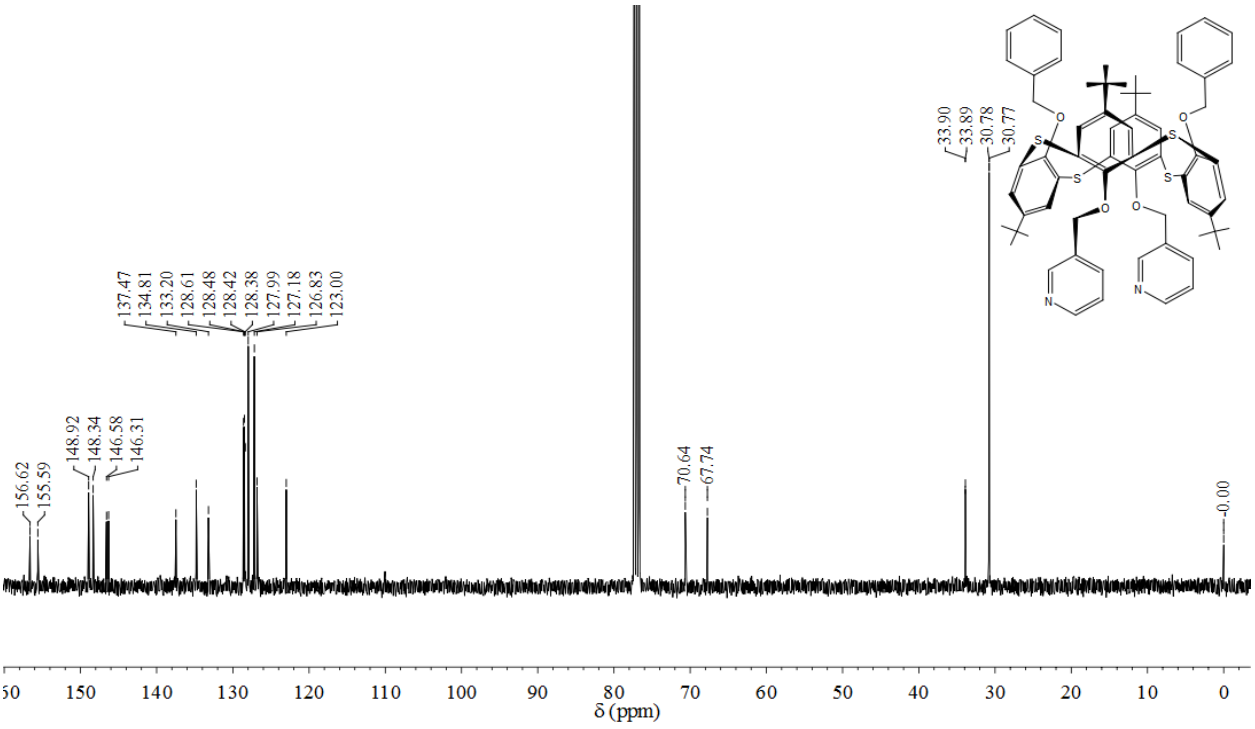

Figure S2. ^{13}C–NMR spectrum of compound **3** (100 MHz, $CDCl_3$, 293 K).

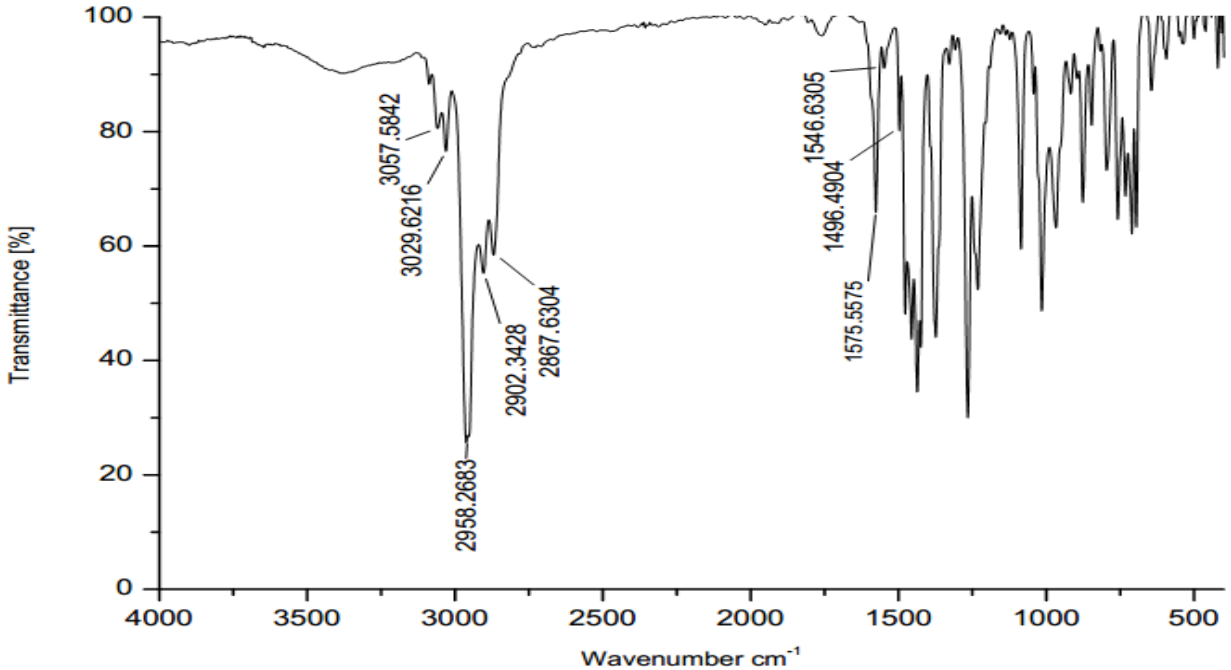

Figure S3. IR spectrum of compound **3**.

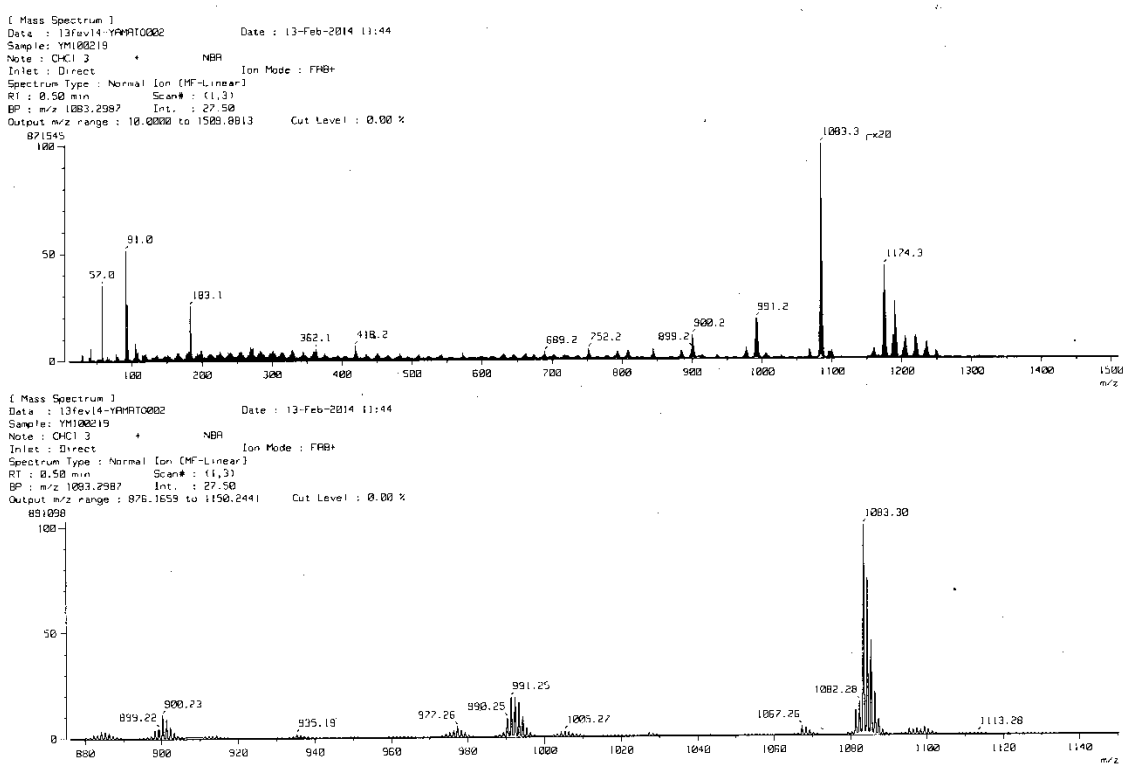

Figure S4. Mass spectrum of compound **3**.

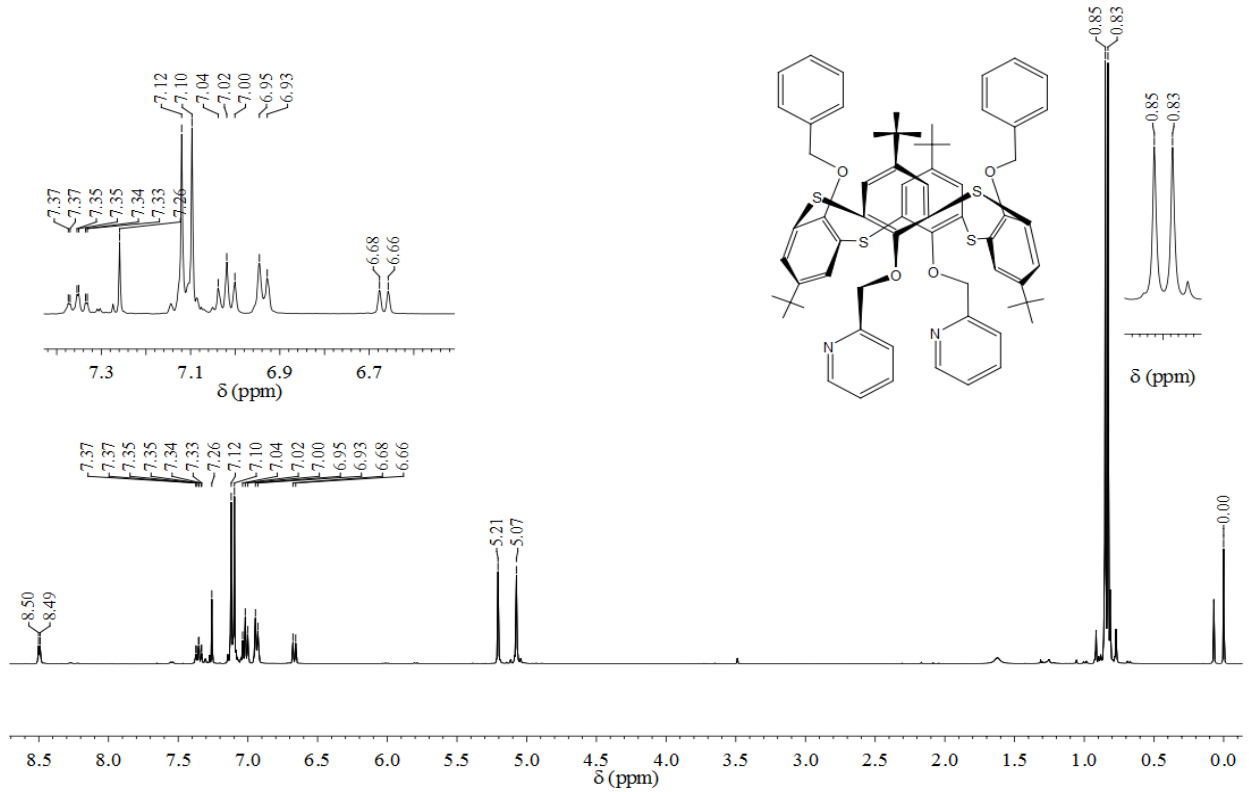

Figure S5. ^{1}H–NMR spectrum of compound **2** (400 MHz, $CDCl_3$, 293 K).

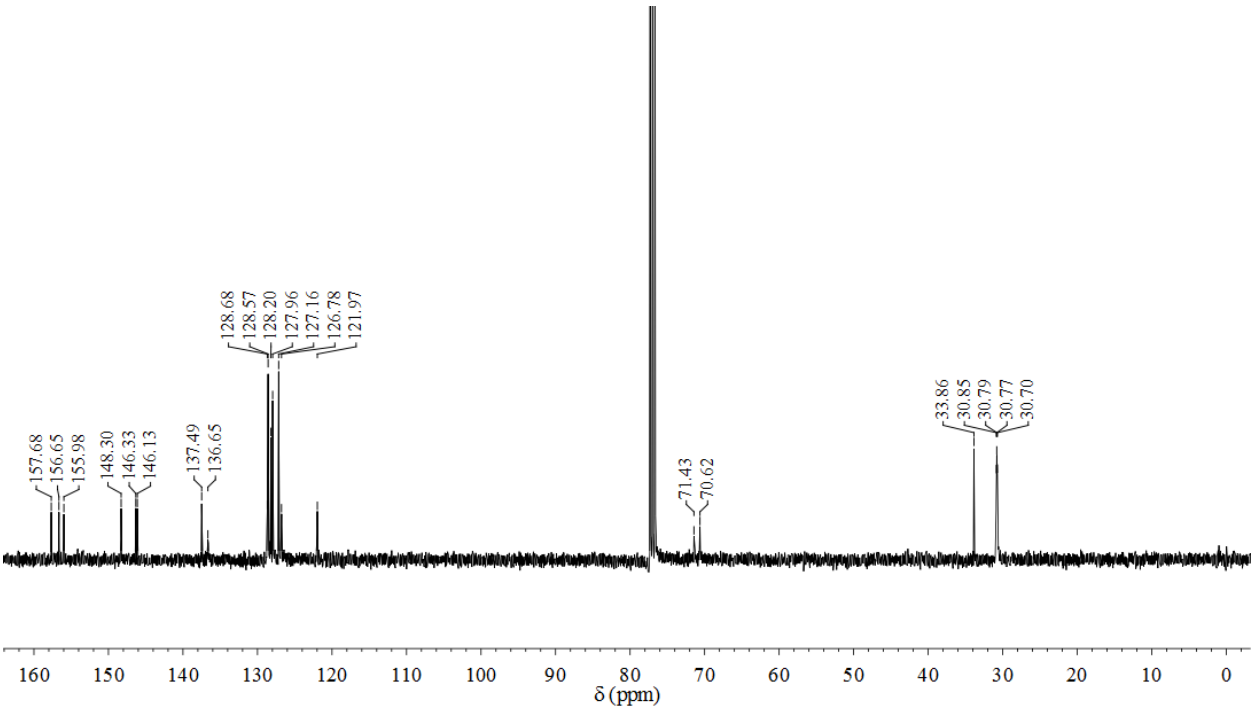

Figure S6. ^{13}C–NMR spectrum of compound **2** (100 MHz, $CDCl_3$, 293 K).

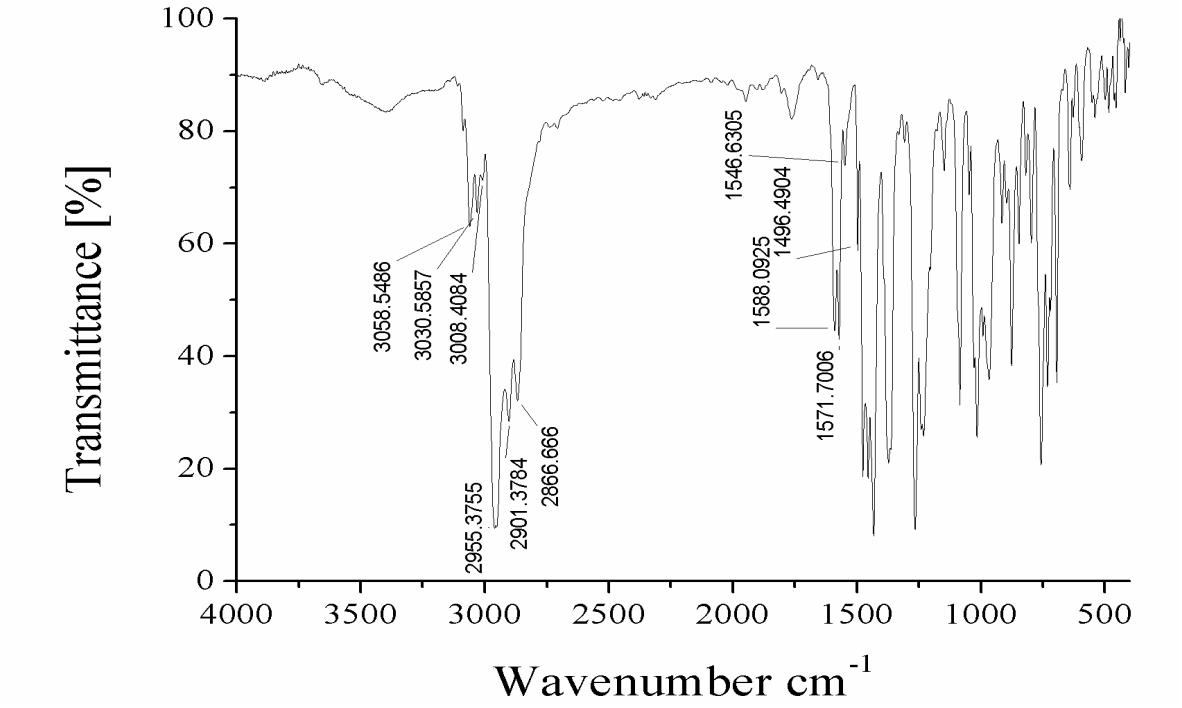

Figure S7. IR spectrum of compound **2**.

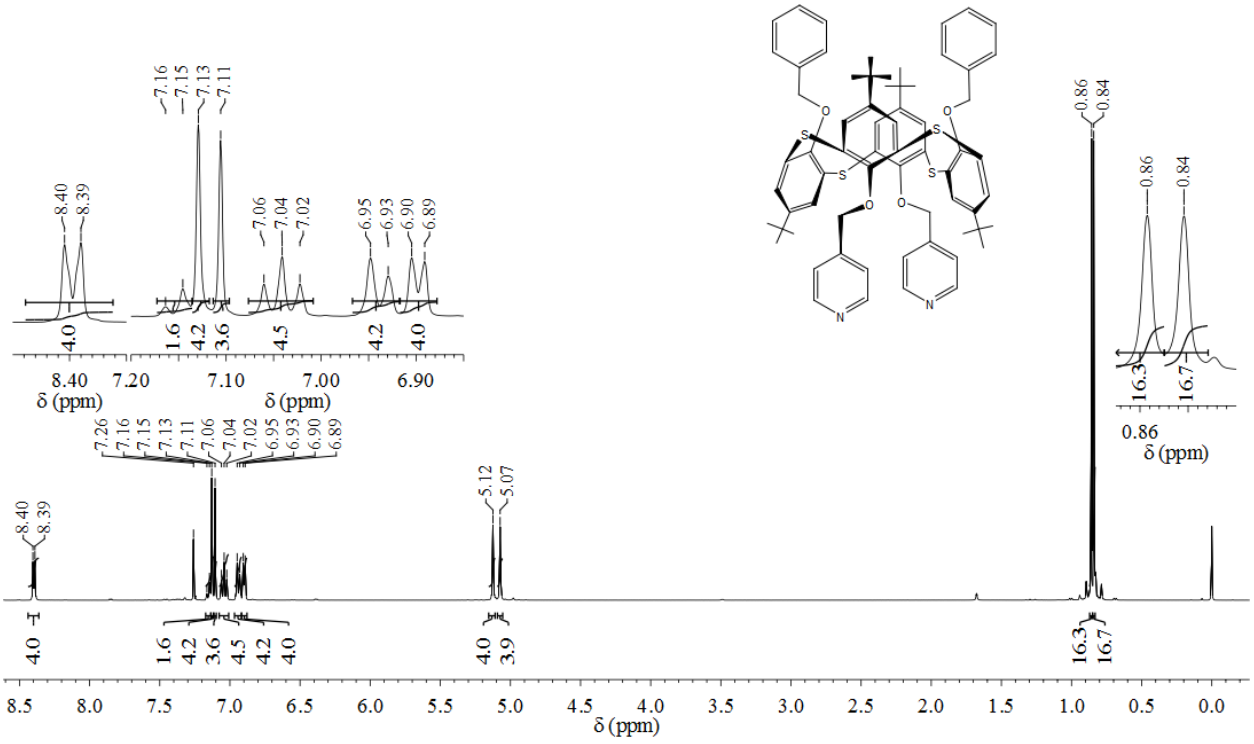

Figure S8. ^{1}H–NMR spectrum of compound **4** (400 MHz, $CDCl_3$, 293 K).

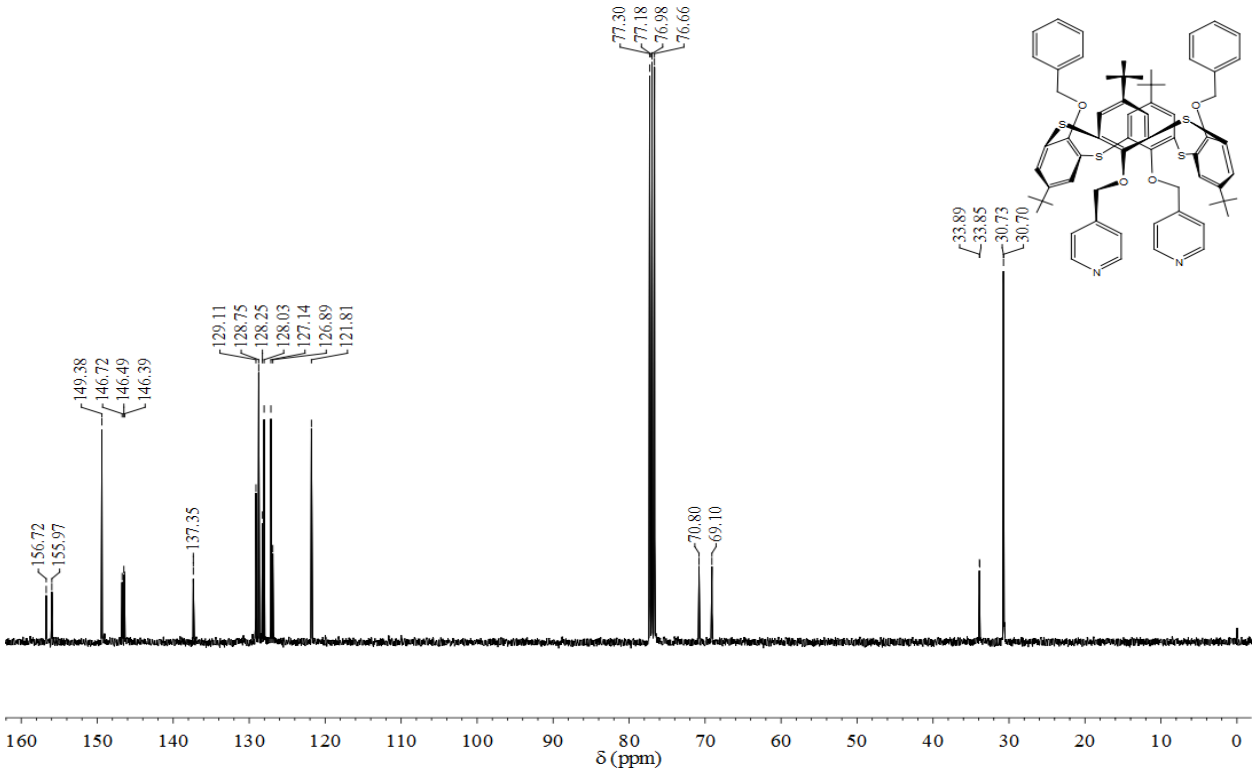

Figure S9. ^{13}C–NMR spectrum of compound **4** (100 MHz, $CDCl_3$, 293 K).

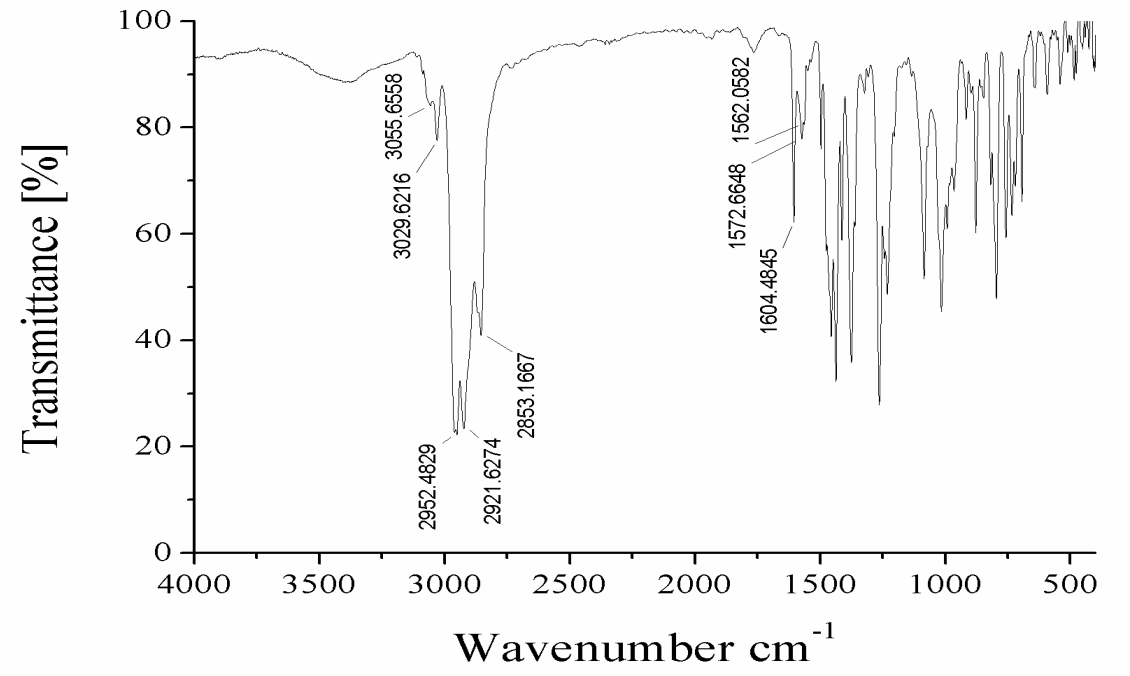

Figure S10. IR spectrum of compound **4**.

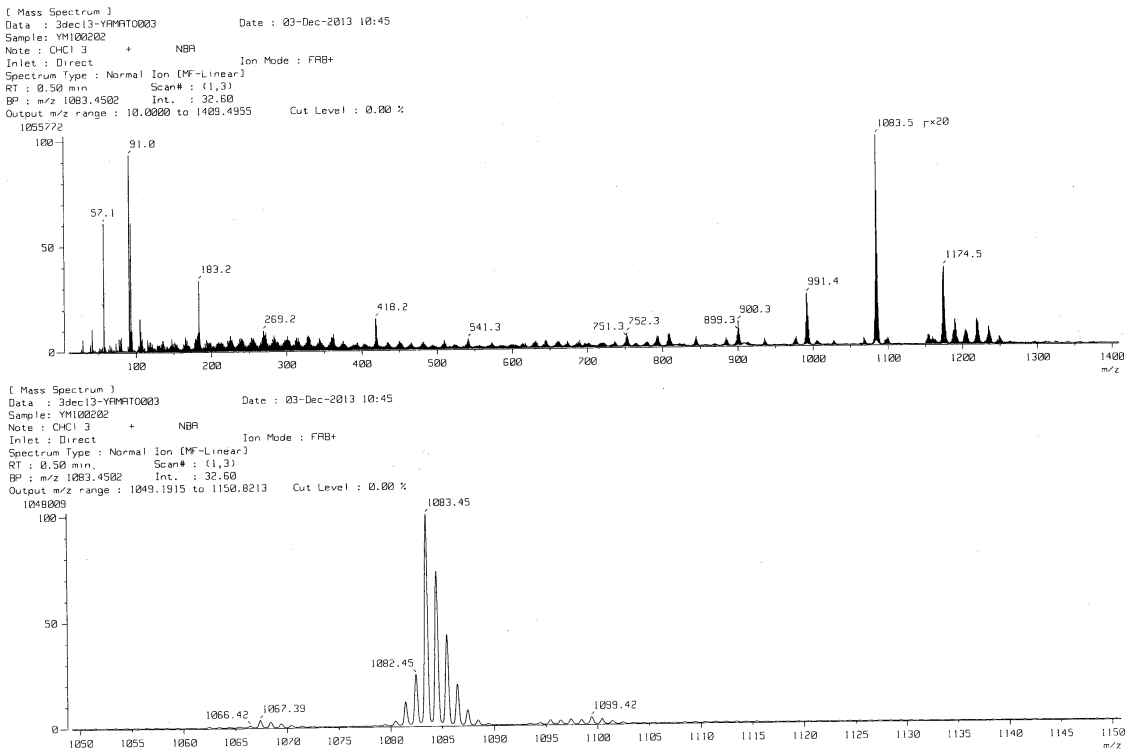

Figure S11. Mass spectrum of compound **4**.

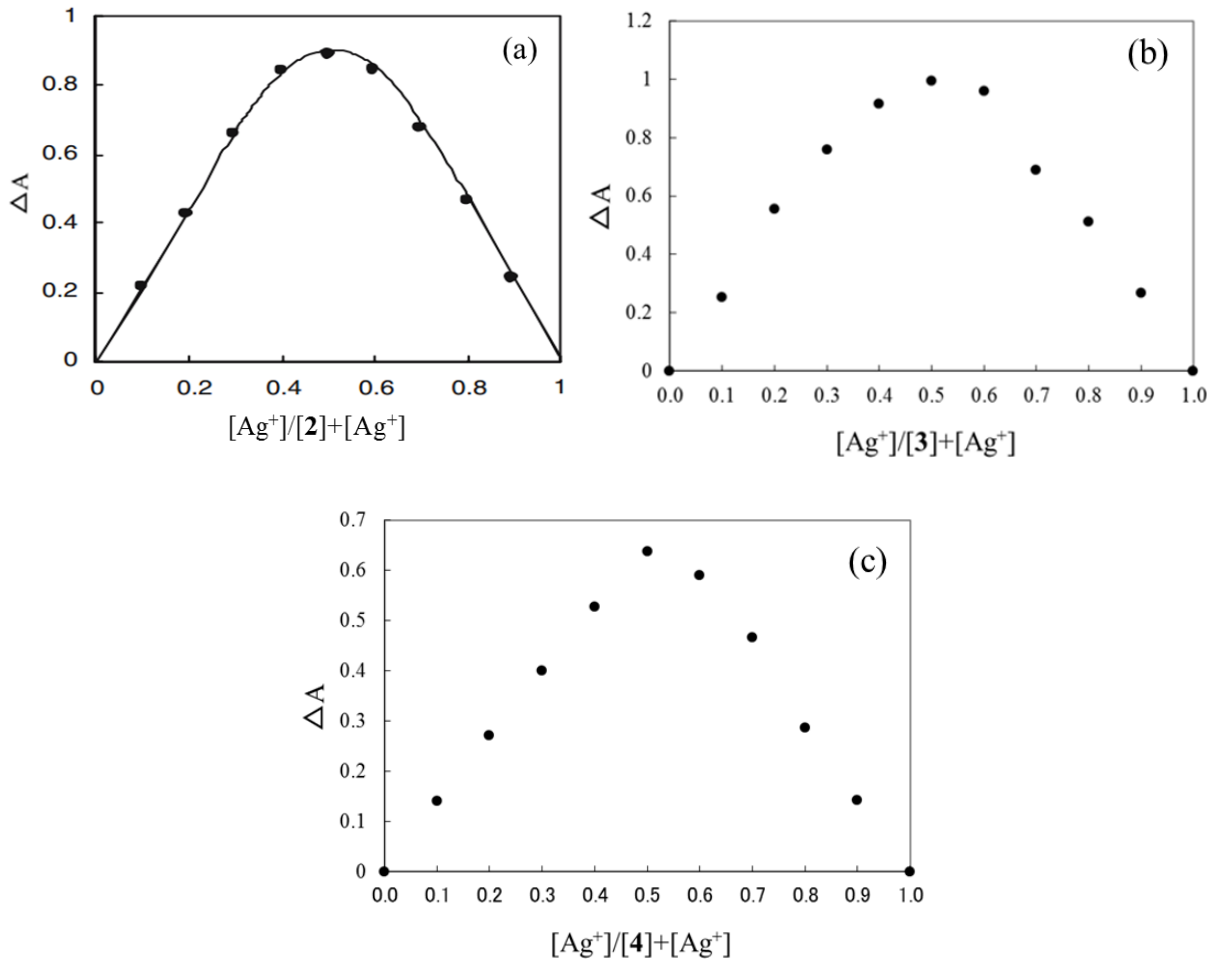

Figure S12 Job's plot for complexation of (a)[1] **2** with Ag^+, (b) **3** with Ag^+ ion and (c) **4** with Ag^+ ion.

Reference

1. T. Yamato, C. P. Casas, H. Yamamoto, M. R. J. Elsegood, S. H. Dale and C. Redshaw, *J. Incl. Phenom. Macrocycl. Chem.*, 2005, **54**, 261–269.

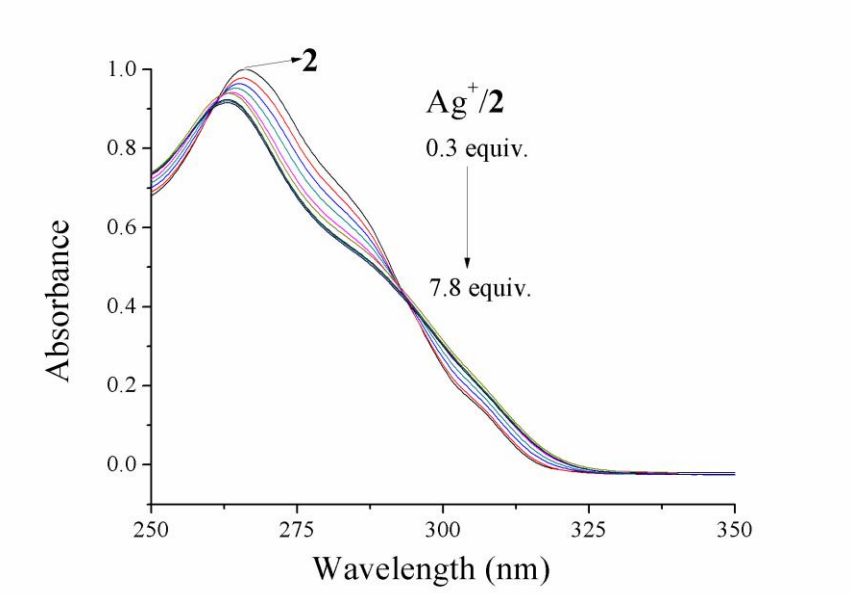

Figure S13 UV titration studies of **2** (1.5 $\times 10^5$ M/L) upon addition of $AgClO_4$ in $CHCl_3$.

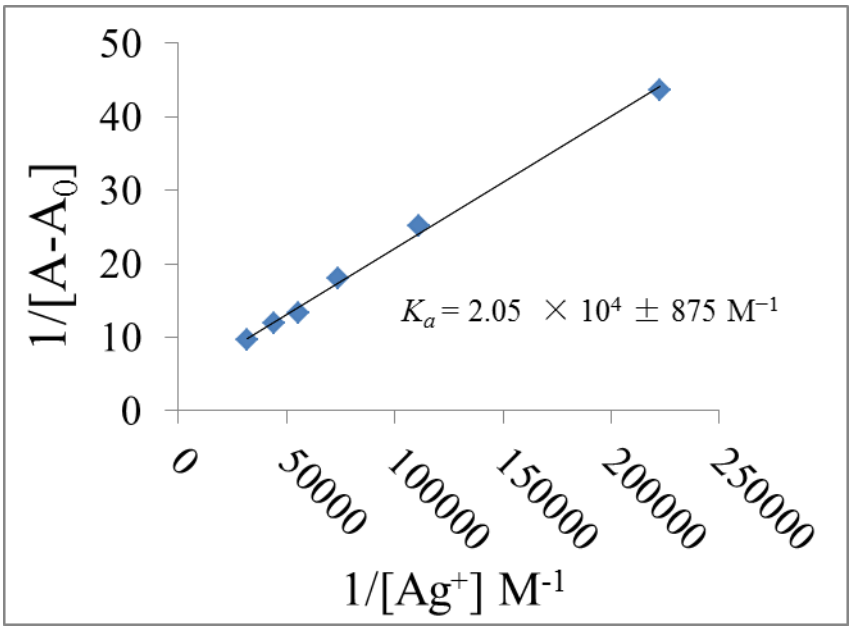

Figure S14 Bensei-Hilderbrand plot of **2** for various concentrations of Ag^+ ion at 298 K. The associate constant (*K*a) was calculated to be 2.05 $\times 10^4 \pm 875$ M^{-1}.

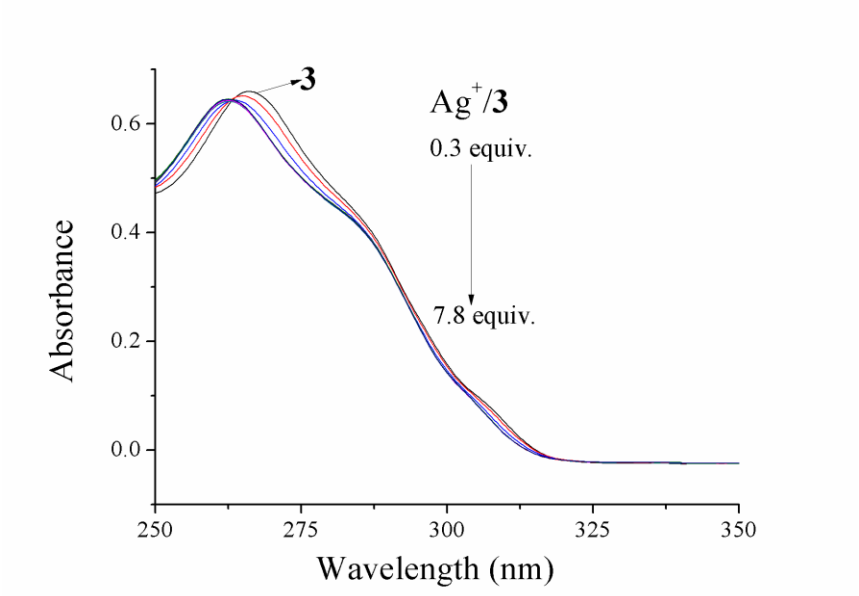

Figure S15 UV titration studies of **3** (1.5 $\times 10^5$ M/L) upon addition of $AgClO_4$ in $CHCl_3$.

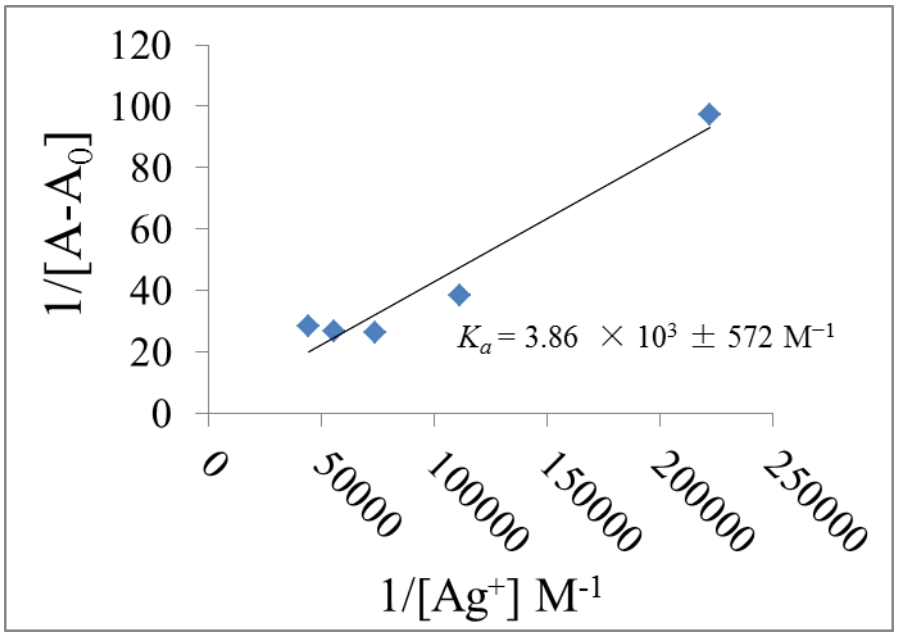

Figure S16 Bensei-Hilderbrand plot of **3** for various concentrations of Ag^+ ion at 298 K. The associate constant (*K*a) was calculated to be 3.86 $\times 10^3$ ± 572 M^{-1}.

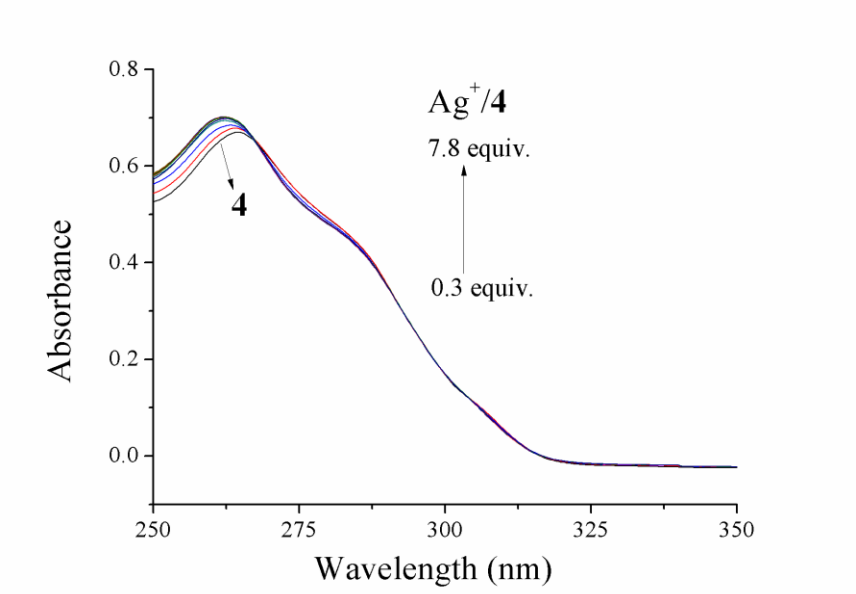

Figure S17 UV titration studies of **4** (1.5 $\times 10^5$ M/L) upon addition of $AgClO_4$ in $CHCl_3$.

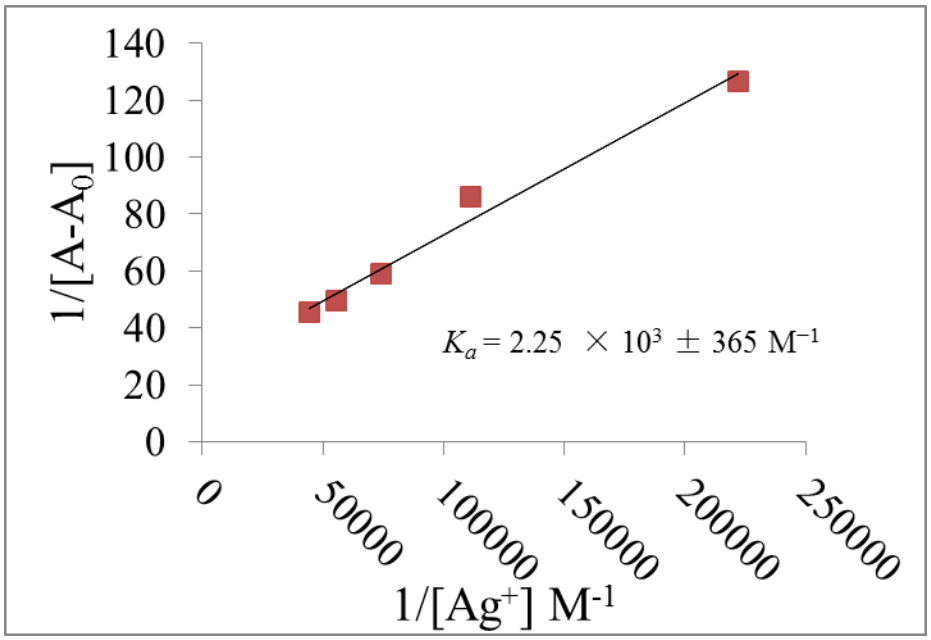

Figure S18 Bensei-Hilderbrand plot of **4** for various concentrations of Ag^+ ion at 298 K. The associate constant (*K*a) was calculated to be 2.25 $\times 10^3$ $\pm$365 M^{-1}.

General Description for Computational Study:

To better understand the binding properties of receptors **2**–**4** with Ag^+, a computation study was carried out. The molecular geometry of the individual structures in the gas-phase were fully optimized using Gaussian09,[2] with the B3LYP level of DFT and the lanl2dz basis set. Significant conformational changes were observed for the pyridine ring protons of **2**–**3** after the complexation with Ag^+. The conformation changes for **2** upon complexation with Ag^+ ion can be seen in Fig. S1 and. Fig. S2. Fig. S1 shows the structure (*right*) of the **2**⊃Ag^+ complex. The optimized molecular geometry suggests that the Ag^+ binds, in accord with the ^{1}H NMR complex study, via a N---Ag^+---S short contact distance bond, which results in the conformation change. The N---N distance between the pyridine nitrogen atoms decreases from 8.001 to 3.761 (Å) (Table 1) since the nitrogen atoms move inwards after complexing with the Ag^+. All four bridge sulphur atoms are roughly the same distance from the Ag^+ and presumably take an equal part in the coordination bonding. However, a different phenomenon was observed in the complexation of **3** with Ag^+. The N--N distance between the pyridine nitrogen atoms decreases from 9.305 to 4.234 (Å) after complexing with the Ag^+ (Fig. S3 and Fig. S4). A similar inference can also be made for the **4**⊃Ag^+complex (Fig. S5 and Fig. S6). The distance between the pyridine nitrogen atoms decrease from 10.138 to 3.798 (Å) (Table 1) after complexation with Ag^+. The optimized molecular geometry suggests that complexation of **3**–**4** with Ag^+ occurs via a N---Ag^+ short contact distance bond, which results in the conformation change.

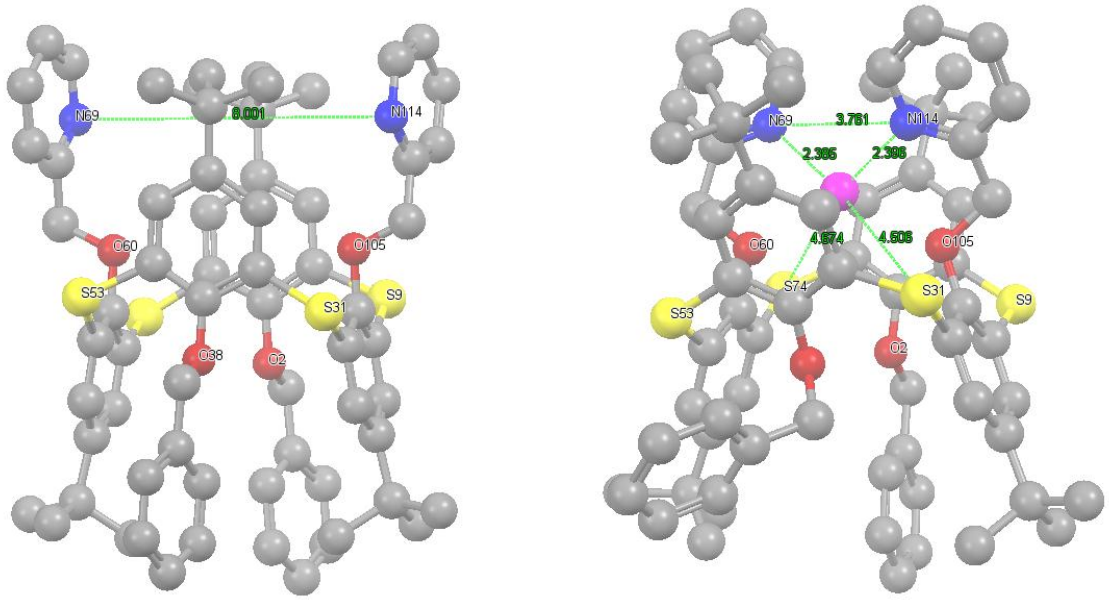

Figure S19. Geometry-optimized (ball and stick) structures of: *Left*: **2** and *Right*: **2**⊃Ag^+complex. Color code for Ag^+ = magenta, pyridine nitrogen = blue, sulphur = yellow and oxygen atom = red. Hydrogen atoms have been omitted for clarity.

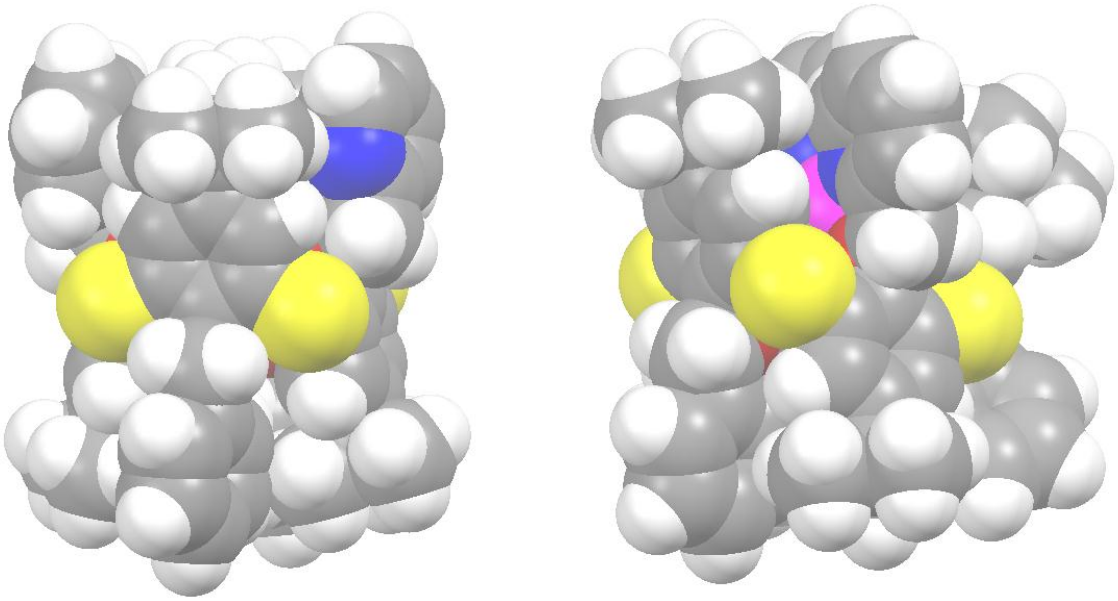

Figure S20. Geometry-optimized (space fill) structures of: *Left*: **2** and *Right*: **2**⊃Ag^+complex. Color code for Ag^+ = magenta, pyridine nitrogen = blue, sulphur = yellow and oxygen atom = red. Hydrogen atoms have been omitted for clarity.

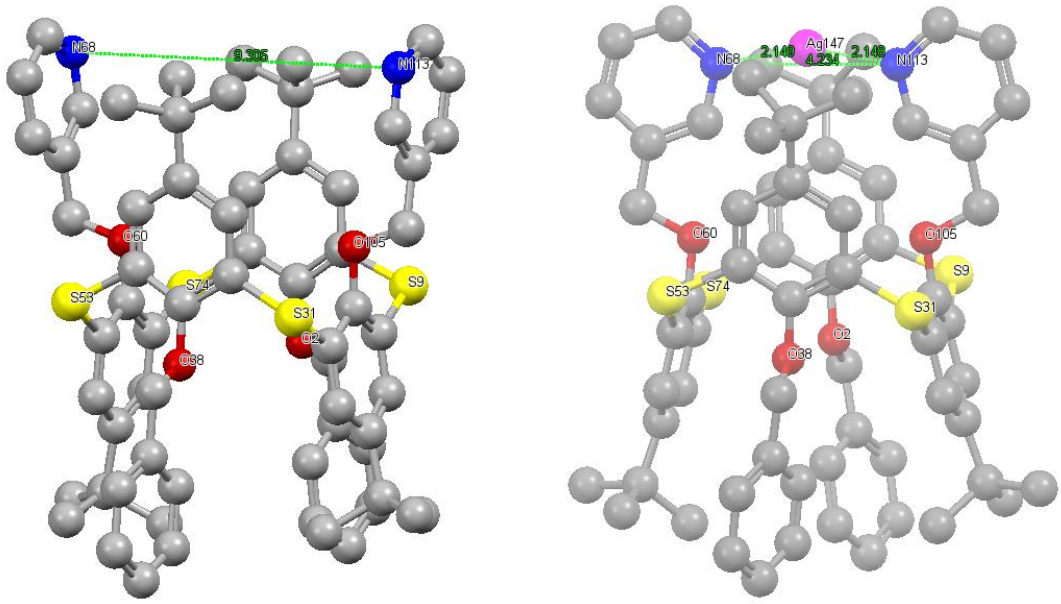

Figure S21. Geometry-optimized (ball and stick) structures of: *Left*: **3** and *Right*: **3**⊃Ag^{+}complex. Color code for Ag^{+} = magenta, pyridine nitrogen = blue, sulphur = yellow and oxygen atom = red. Hydrogen atoms have been omitted for clarity.

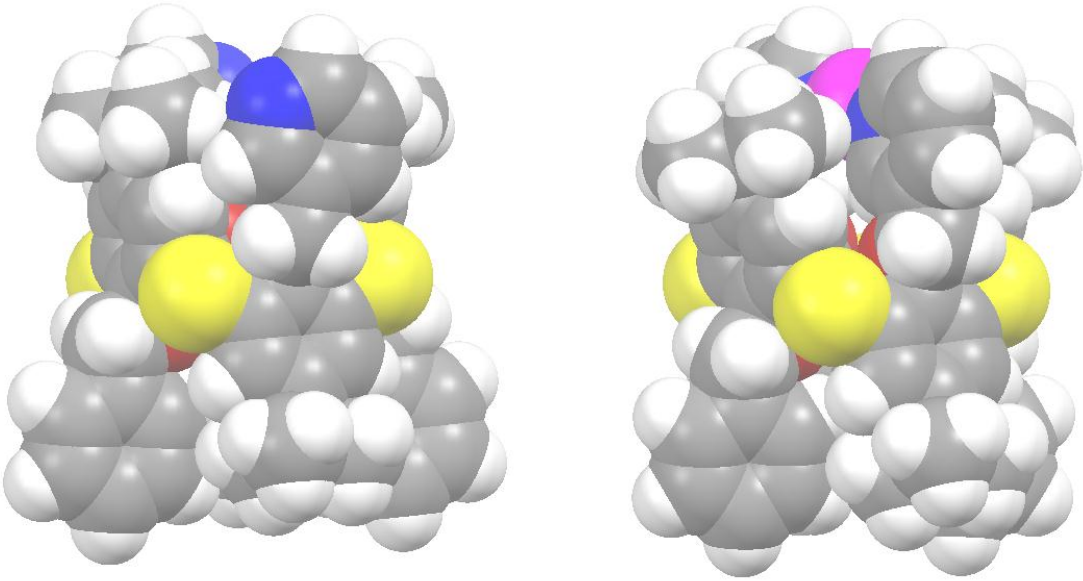

Figure S22. Geometry-optimized (space fill) structures of: *Left*: **3** and *Right*: **3**⊃Ag^{+}complex. Color code for Ag^{+} = magenta, pyridine nitrogen = blue, sulphur = yellow and oxygen atom = red. Hydrogen atoms have been omitted for clarity.

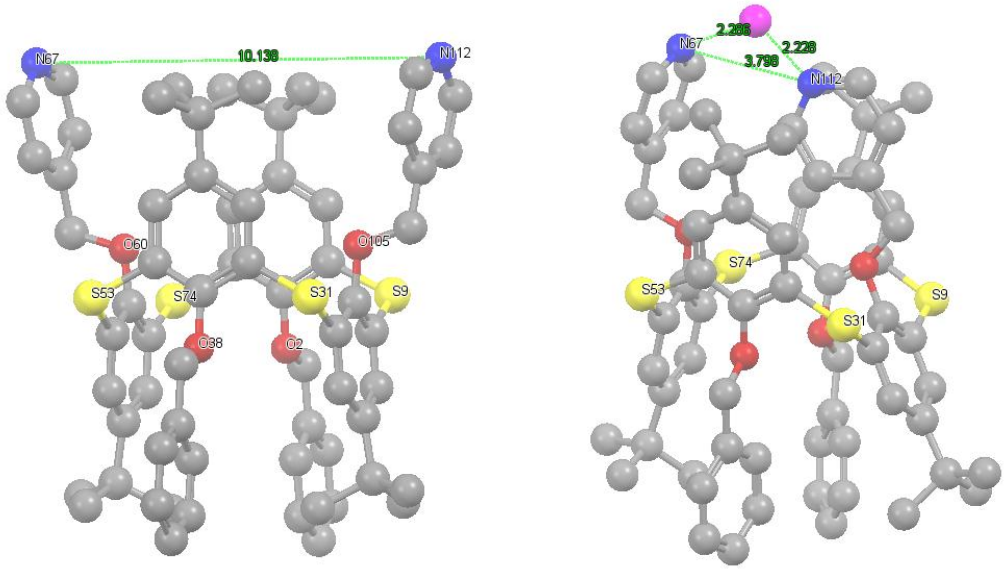

Figure S23. Geometry-optimized (ball and stick) structures of: *Left*: **4** and *Right*: **4**⊃Ag^+complex. Color code for Ag^+ = magenta, pyridine nitrogen = blue, sulphur = yellow and oxygen atom = red. Hydrogen atoms have been omitted for clarity.

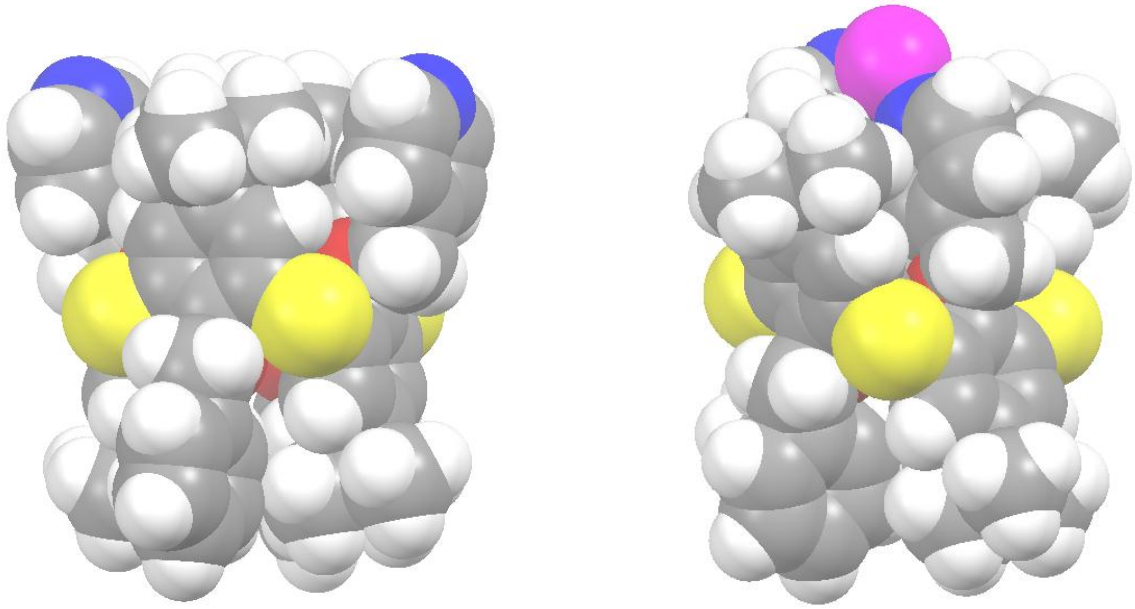

Figure S24. Geometry-optimized (space fill) structures of: *Left*: **4** and *Right*: **4**⊃Ag^+complex. Color code for Ag^+ = magenta, pyridine nitrogen = blue, sulphur = yellow and oxygen atom = red. Hydrogen atoms have been omitted for clarity.

Table S1 The calculated distance for selected parameters for the backbones of the 1,3-*alternate*-**2**–**4** and their complexes with Ag^+ optimized at B3LYP/ lanl2dz level(Distance in Å).

Parameter	**2** (Å)	**2**⊃Ag^+ (Å)	Parameter	**3** (Å)	**3**⊃Ag^+ (Å)	Parameter	**4** (Å)	**4**⊃Ag^+ (Å)
N_{69}-N_{114}	8.001	3.761	N_{68}-N_{113}	9.305	4.234	N_{67}-N_{112}	10.138	3.798
N_{69}-S_9	8.188	6.841	N_{68}-S_9	6.715	7.651	N_{67}-S_9	10.536	9.319
N_{69}-S_{31}	8.89	6.712	N_{68}-S_{31}	6.219	7.941	N_{67}-S_{31}	9.96	9.249
N_{69}-S_{53}	5.614	5.231	N_{68}-S_{53}	9.431	5.966	N_{67}-S_{53}	6.528	6.713
N_{69}-S_{74}	5.036	4.708	N_{68}-S_{74}	9.971	6.12	N_{67}-S_{74}	7.3	6.762
N_{114}-S_9	5.614	5.512	N_{113}-S_9	9.431	5.953	N_{112}-S_9	6.528	6.942
N_{114}-S_{31}	5.036	4.323	N_{113}-S_{31}	9.971	6.132	N_{112}-S_{31}	7.3	6.84
N_{114}-S_{53}	8.188	6.556	N_{113}-S_{53}	6.715	7.654	N_{112}-S_{53}	10.536	7.055
N_{114}-S_{74}	8.89	6.886	N_{113}-S_{74}	6.219	7.924	N_{112}-S_{74}	9.96	7.111
N_{69}-Ag^+	-	2.385	N_{68}-Ag^+	-	2.149	N_{67}-Ag^+	-	2.286
N_{114}-Ag^+	-	2.396	N_{113}-Ag^+	-	2.148	N_{112}-Ag^+	-	2.228
S_9-Ag^+	-	4.98	S_9-Ag^+	-	6.811	S_9-Ag^+	-	8.857
S_{31}-Ag^+	-	4.506	S_{31}-Ag^+	-	7.069	S_{31}-Ag^+	-	8.749
S_{53}-Ag^+	-	4.699	S_{53}-Ag^+	-	6.818	S_{53}-Ag^+	-	7.725
S_{74}-Ag^+	-	4.674	S_{74}-Ag^+	-	7.056	S_{74}-Ag^+	-	7.8

Calculated binding energies

The DFT B3LYP/ lanl2dz basis set-calculated binding energies (ΔE) of the Ag^+ complexes of thiacalix[4]arene derivatives **2-4** ($L_{free} + Ag^+_{free} \rightarrow L/Ag^+_{complex}$) formed between the Ag^+ ion and the free thiacalix[4]arene derivatives **2-4** in the gas phase at 298 K are based on the equation (1), are listed in Table S2.

For this system, the binding energy ΔE can be express as follows:

$$\Delta E = E(L/Ag^+_{complex}) - E(L_{free}) - E(Ag^+_{free}) \qquad (1)$$

Table S2 Calculated binding energies for the thiacalix[4]arene derivatives with Ag^+.

Parameter	**2**⊃**Ag**$^+$ ΔE (KJ/mole)	**3**⊃**Ag**$^+$ ΔE (KJ/mole)	**4**⊃**Ag**$^+$ ΔE (KJ/mole)
Binding energy for thiacalix[4]arene derivatives with **Ag**$^+$	-488.096	-464.022	-372.966

Reference

2. M. J. Frisch, G. W. Trucks, H. B. Schlegel, G. E. Scuseria, M. A. Robb, J. R. Cheeseman, G. Scalmani, V. Barone, B. Mennucci, G. A. Petersson, H. Nakatsuji, M. Caricato, X. Li, H. P. Hratchian, A. F. Izmaylov, J. Bloino, G. Zheng, J. L. Sonnenberg, M. Hada, M. Ehara, K. Toyota, R. Fukuda, J. Hasegawa, M. Ishida, T. Nakajima, Y. Honda, O. Kitao, H. Nakai, T. Vreven, Jr. J. A. Montgomery, J. E. Peralta, F. Ogliaro, M. Bearpark, J. J. Heyd, E. Brothers, K. N. Kudin, V. N. Staroverov, T. Keith, R. Kobayashi, J. Normand, K. Raghavachari, A. Rendell, J. C. Burant, S. S. Iyengar, J. Tomasi, M. Cossi, N. Rega, J. M. Millam, M. Klene, J. E. Knox, J. B. Cross, V. Bakken, C. Adamo, J. Jaramillo, R. Gomperts, R. E. Stratmann, O. Yazyev, A. J. Austin, R. Cammi, C. Pomelli, J. W. Ochterski, R. L. Martin, K. Morokuma, V. G. Zakrzewski, G. A. Voth, P. Salvador, J. J. Dannenberg, S. Dapprich, A. D. Daniels, O. Farkas, J. B. Foresman, J. V. Ortiz, J. Cioslowski, D. J. Fox. *Gaussian 09, Revision D.01*; Gaussian, Inc., Wallingford CT, 2013.